



Efficient ML Technique for Brain Tumor Segmentation, and Detection, based on MRI Scans Using Convolutional Neural Networks (CNNs)

Nasir Ayub^{1*}

Deputy Head of Engineering Calrom Limited, M1 6EG, United Kingdom
Department of Computer Science, Faculty of Computer Science & IT
Superior, University Lahore, 54000, Pakistan. Corresponding Author Email:

snasir.ayyub@hotmail.com

Muhammad Waqas Iqbal²

Department of Information Technology, Bahria University, Islamabad

Informtowaqas@gmail.com

Muhammad Usman Saleem³

Department of Computer Science, Government College Women
University Sialkot. usman.saleem@gcwus.edu.pk &

usman.saleem@live.com

Muhammad Nabeel Amin⁴

Riphah International University, Faisalabad. nabeelofficial70@gmail.com

Osama Imran⁵

Department of Computer Science, COMSATS University
Islamabad, Lahore Campus. osamaimran135@gmail.com

Hamayun Khan⁶

Department of Computer Science, Faculty of Computer Science & IT
Superior, University Lahore, 54000, Pakistan.

hamayun.khan@superior.edu.pk

Abstract

Experts need accurate segmentation and detection alongside the classification of Brain tumors from MRI images because this approach helps identify neurological problems early for timely treatment. Deep learning technology has made Convolutional Neural Networks (CNNs) effective in analyzing complex medical imaging challenges by developing automatic abilities to detect and categorize complex data features. This study used 1,251 Brain Tumor MRI images from BraTS2021



for model testing of CaPTk, 2DVNet, EnsembleNets, and ResNet50 towards brain tumor segmentation. The research utilized the DSC and HD metrics for its evaluation process. Importantly, EnsembleUNets achieved the minimum HD of 18 while reaching the maximum DSC of 0.92. The analysis of the radiomic feature confirmed that EnsembleUNets delivered the best CCC value at 0.75 together with the lowest RMSE at 0.52 and the highest TDI at 1.9 for tumor segmentation and classification in clinical practice. These findings show EnsembleUNets effectively perform brain tumor segmentation and classification and identification so healthcare professionals now have more effective guidance about implementing CNN-based clinical applications.

Keywords: Cyber-physical systems (CPSs). Security Protocols, Encryption, OpenVPN, IKEv2/IPsec, WireGuard, Quantum Computing

Introduction

Most kinds of prime brain tumors bring about fatal consequences to human life. Brain malignancies originating from other body parts tend to metastasize to the brain while primary brain tumors develop internally within brain tissues. The correct visualization of tumors serves as a fundamental requirement for their medical diagnosis. These tumors need essential diagnostic imaging for their proper assessment [1, 2]. MRI together with CT and PET scans represent standard high-resolution techniques used in medical practice. The investigation of brain structure requires MRI assessments because this method serves as the primary tool for brain tumor identification along with their evaluation [3, 4]. Brain cancers have their origins either inside the brain tissue (primary) or outside the brain origin (secondary) before spreading to the brain. MRI stands as a non-invasive imaging method that enables patients to receive a diagnosis through its broad usage for brain assessment. The machine generates images of different body segments by processing waves and electronic signals. The moveable bed represents an essential



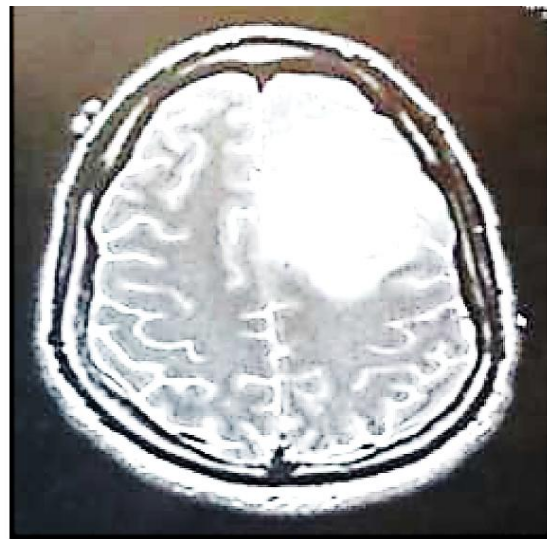
part of the cylindrical framework containing the MRI unit that has magnets surrounding its whole perimeter. Magnetic access at the entry point leads patients to table-based movement into the scanning area for their MRI exam [5, 6]. The patient-enclosed space utilizes an intense magnetic field to reorient hydrogen atom protons. The examination technology generates body images by converting radio wave signals that enter the body with its embedded protons [7].

Temporal Analysis

The modern consumer market needs personalized products because customers now possess numerous options. Doctors use favorable magnetic fields and radio signals to produce imaging pictures that display body growth changes through MRI technology. Image segmentation functions as a process to divide pictures into their maximum basic units including pixels and their elements [8, 9]. To operate this technique medical professionals convert pixels of a region into identifiable clusters based on their color intensity and texture parameters. The resulting images provide enhanced view capabilities when body structures slightly change [10]. The small structures inside the human body become visible to medical experts through vivid details enabled by MRI technology in biomedicine. This technology approaches tissue detection with better capability than conventional imaging approaches and serves to uncover tissue variations. For many years radiologists dedicated extensive time to inspecting MRI scans before determining the presence of brain tumors [11, 12]. A great deal of research dedicated to image segmentation has taken place throughout the previous several decades resulting in numerous completed studies. The picture of the brain in MRI appears in Figure 1 together with Brain scan results both with and without tumor. A better diagnostic process emerges through an MRI Scan examination.



(a)



(b)

Figure 1: MRI Images (a) with Tumor and without Tumor [13]

Related Work

This section reviews recent studies about deep learning methods in brain illness detection through the investigation of CNN techniques for brain tumor MRI scan segmentation. Several research works utilize CNNs to develop methods that segment brain tumors. The 3D CNN model proposed by Urban demonstrated successful tissue class prediction through 3D patches used as inputs when working on multimodal MRI glioma segmentation [14, 15]. The researcher generated a technique to convert 4D medical data into 2D image patches to allow 2D-CNN networking for brain tumor segmentation. The previous research projects implemented various CNN architectures to perform brain tumor segmentation [16]. They designed a CNN to predict component classifications of multi-level data structures through a two-stage training system that addresses class imbalance. Rao obtained features from MRI modality images using four unique CNN architectures while fixing multiple plane settings per pixel. Researchers in recent times presented new CNN architectural frameworks for conducting brain tumor segmentation [17].



Brain MRI Classification

The researchers established a CNN-based Classification that bridges understanding of both wide brain tissue contextual information and precise brain MRI details. Three different CNN-based glioma segmentation approaches have been suggested for brain tumor segmentation while using smaller 3x3 estimated channels during convolutional phases [18]. Multiple researchers explored different methods that combine multi-view knowledge-based collaborative deep learning with hybrid CNN-DWT-LSTM approaches to segment and classify brain tumors. During the last ten years, CNNs have increasingly emerged as a popular deep-learning approach for medical imaging applications. Multiple research studies prove the ability of CNNs to discover medical anomalies such as cancers in different human organs [19]. Research activities in segmentation continue because different methods lack a complete evaluation system. The fundamental goal of 2D MRI data is to perform precise tissue separation of brain areas and tumors. Great success in defining tumor boundaries depends on MATLAB software methods along with supplementary tools [20, 21]. The segmentation process has three significant categories including manual approaches alongside half-automatic and completely automatic methods.

The need for manual segmentation has declined as radiologists analyze MRI images with expert analysis to perform their work although the process takes a long time and errors are likely to happen. Users must provide inputs during semi-automatic method execution for labeling tasks while the methodology struggles to produce steady results [22, 23]. The research studies demonstrate how deep learning techniques perform the detection and segmentation of multiple brain diseases. This paper analyzes in depth how CNN methodology styles detect brain diseases [24, 25]. The earliest artificial neural network research



established deep learning through perceptron models that were created first [26]. The linear classifier marked the start of computerized learning method development. The analysis of non-linear data caused neural networks to lose popularity for multiple years. Deep learning originated as neural networks obtained advancement by bigger data availability updated training methods and enhanced computing power. Neural networks perform automatic data feature extraction because it is a machine learning technique that uses different layered models to recognize patterns starting from basic to advanced. CNNs along with RNNs represent the most ubiquitous choices from existing neural network frameworks. Image and video recognition change because CNNs duplicate the visual cortex's organizational design [27, 28]. The majority of contemporary research emphasizes automatic methods that aim at improving the handling of image variability. Traditional computers function differently than neural networks because they imitate brain processing methods. Many interconnected units (neurons) in neural networks employ examples for problem-solving rather than following strict programming algorithms.

High accuracy in automatic segmentation through deep learning methods depends on well-prepared training datasets [29, 30]. Developing trustworthy and efficient tumor detection methods using CNN technology remains the main research focus. The task of segmenting brain tumors from preoperative MRI scans performed by neuroradiologists becomes challenging because tumors exhibit irregular shapes with indistinct boundaries in addition to scan distortions. The processing duration extends and increases in complexity because of this condition [31, 32]. The medical sector has achieved exceptional results by applying deep learning techniques for automatic tumor segmentation procedures. A CNN architectural structure uses multiple hidden layers for convolution and activation which successfully identifies various diseases



such as skin cancer brain tumors and breast cancer [33, 34]. Many deep learning approaches have proven effective for brain tumor segmentation yet researchers have not conducted a comprehensive evaluation of their accessibility and dependability characteristics. This research responds to a gap by performing an extensive evaluation of the accuracy standards used in widely adopted brain tumor segmentation algorithms. This research evaluates how usable and dependable four popular automated deep learning methods namely CaPTk software, 2DVNet, Ensemble UNets, and ResNet50 for brain tumor segmentation [35, 36].

Convolutional Neural Network

Research about mammalian visual cortex mechanisms formed the basis of Convolutional Neural Networks (CNNs). CNNs reproduce brain functionality which enables neurons to analyze various spatial patterns in visual information [37, 38]. CNN architecture refers to an essential mathematical approach that enables weight sharing along with local processing and spatial pattern retention. The LeNet-5 model created by Kate and Shukla marked the first successful implementation of CNNs for handwritten number detection during the 1980s [39, 40]. Document recognition progressed a great deal after the model introduced gradient-based learning mechanisms. CNNs demonstrate exceptional performance in data arrangements with grid-like structures such as images that equal two-dimensional pixel grids. The study reviewed the foundation of neural networks and their advanced structures alongside their primary medical diagnostic applications [41, 42]. The research explored the historical development of these networks starting with biological prototypes up until their modern applications where CNNs took center stage because of their transformative effects on medical image diagnostics. The review addressed major barriers that involved working with extensive labeled data collections and enhancing model



comprehensibility simultaneously with showing how neural networks have substantially boosted diagnostic precision [43, 44].

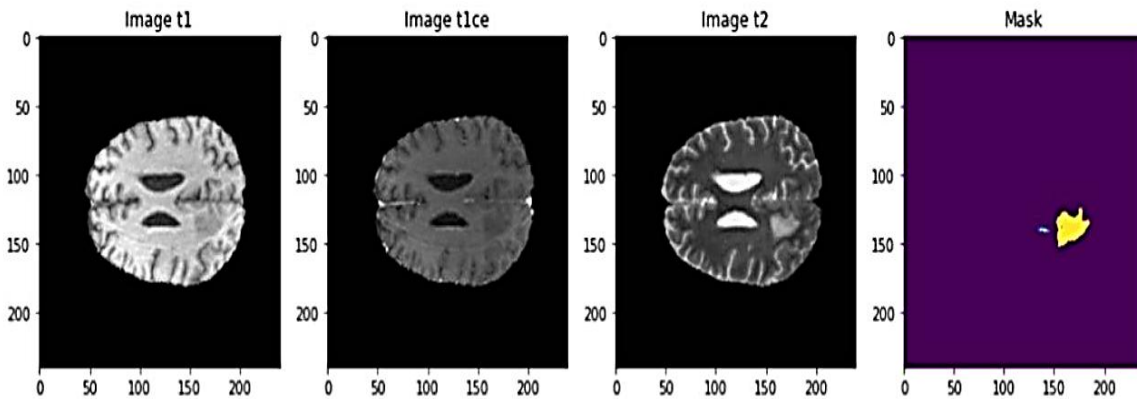


Figure 2: Analysis of (a) Image stage 1, (b) Image stage 2 (a) Image stage 3 and Mask in positive Brain Tumor [45]

The CaPTk brain tumor segmentation module utilizes Deep Medic as its CNN method while basing its training on the BraTS2021 dataset. The brain lesion detection process of Deep Medic depends on an 11-layer deep CNN (Convolutional Neural Network) structure. The network platform operates on three-dimensional images while assessing different size levels. It functions by applying the 3D conditional random field (CRF) to enhance segmentation accuracy according to Deep Medic. The effective identification of brain lesions in medical images becomes achievable through this processing method used by Deep Medic. Each section within the network operates as two parts and utilizes 33 kernels to perform a detailed analysis of 3D image data [46, 47]. The deep 3D multi-scale CNN incorporates a system of two fundamental processing paths. The original setup included 53 kernels but Deep Medic implemented 33 kernels within its pathways. The second pathway compresses the same data after processing by condensing it into a third of its original size which it pursues to the central point together with the first pathway. The compression process allows the system to monitor a wide field that spans 51^3 voxels. The attributes detection process takes place in a 17 space during the final stage of both pathways. This



investigation adopted default command line settings from CaPTk developers when executing the experiment [48, 49].

The Volumetric Convolutional Network (V-Net) focuses on helping medical classification systems by detecting brain tumors from diverse MRI scan data through its image analysis features. The V-Net system has two operational units with the encoder segment placed on the left side and the decoder unit located on the right side. The encoder compresses the signals, while the decoder decompresses them to their original size. Through its processing, V-Net maintains multiple spatial map resolutions and spatial relationship awareness [50, 51].

The developed system reaches high performance and establishes accurate geographical location because lateral connections transfer information between the encoder and decoder. The Parametric Rectified Linear Unit (PReLU) helps V-net recognize patterns in the input data through which it can detect outlines according to known designs. An existing pre-built 2D V-Net model received HGG BraTS2020 dataset training to evaluate study results against alternative models [52, 53]. The CNN-based U-Net model functions as one of the primary choices for executing segmentation tasks in medical picture analysis. U-Net shows outstanding performance when it comes to identifying brain tumors through combining multiple MRI imaging methods. The U-Net design incorporates a sequential operation of decreasing path units to create contextual areas while simultaneously decreasing the scale of detail and increasing the path that utilizes this contextual information to produce high-detailed segmentation results. Developed a sequential system of models that contained 3D U-Net along with 3D MI U-Net and 3D+ 2D MI U-Net ensemble model. In the third model, all 2D slices together with the second model outputs operate while the first model works with 3D MRI image patches. An integrated integration of these three models enhances the accuracy of segmentation results as a result of their



combined application. This study applied the specified pre-trained model as its foundation [54, 55]. The brain MRI scan segmentation particularly depends on ResNet50 as one of its several models used for image separation functions. TensorFlow/Kera's frameworks utilize the original ResNet50 model which contains skip connections in residual blocks allowing the model to train while operating independently from large prediction to ground truth mismatches. The architecture contains 50 layers which makes it larger than the models with 18 and 34 layers such as ResNet18 and ResNet34. The picture classification system together with extractive features deploys ResNet50 because it demonstrates excellent performance. We used ResNet50 which has undergone prior training for tumor segmentation of BraTS2020 brain MRI scan data. CSV logger was used as part of process checking during training while ReduceLROnPlateau was used for learning rate optimization [56].

Method & Materials

Convolution Neural Network-based Brain Tumor Segmentation (CNNBTS)

The local objective function of the i -th client is denoted by $f_i(t)$ while x represents the current model parameter and ξ indicates the data point sampled for local training. In these assumptions LOF represents local and SOF demonstrates second-order function smoothness and LH stands for Lipschitz convexity. Lastly, SCOF and COF express objective function convexity while $f(x_1) \geq f(x_2) + (x_1 - x_2)^T \nabla f(x_2)$ indicates the coercive property and CF denotes the existence of a global minimum. BG, BV along BGD determine conditions required to prove convergence. The function characteristics of convexity in MOG are described by two properties: first SCOF and COF while second $f(x_1) \geq f(x_2) + (x_1 - x_2)^T \nabla f(x_2)$ establishes the rules of convexity and the coerciveness of $f(x)$ follows a pattern of $\lim_{x \rightarrow \infty} f(x) \rightarrow \infty$. When CF applies it guarantees



the existence of a worldwide minimum for the objective function. The properties of gradients are captured through BG, BV, and BGD. This situation emphasizes the need to combine technological expertise with legal and ethical considerations when approaching such problems. The Proposed Technique relies on the following algorithm.

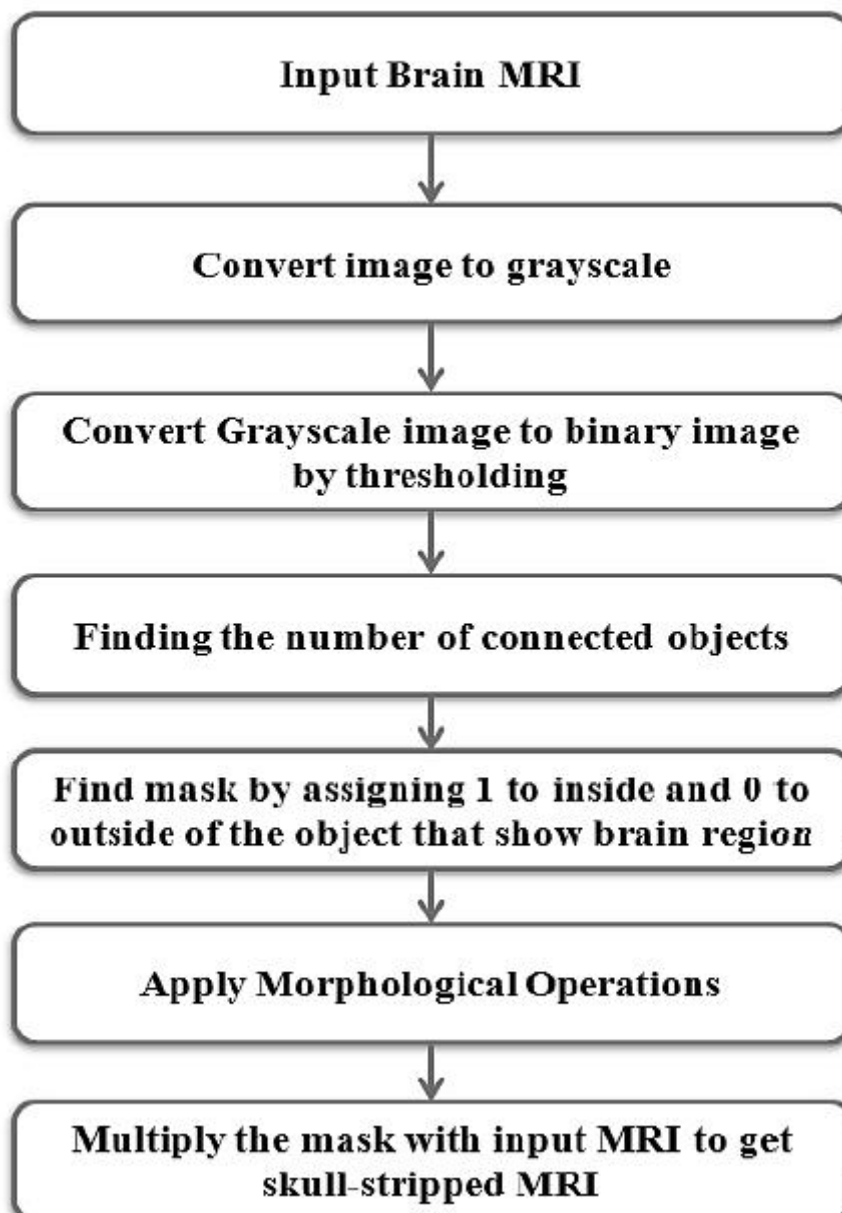


Figure 3: Framework for Skull Segmentation

Data Description

The research works with data obtained from the RSNA-ASNR-MICCAI Brain Tumor Segmentation Challenge 2021. BraTS2021 provides medical



scans from 2000 participants obtained through TCGA-GBM and TCGA-LGG in addition to Ivy-GAP and CPTAC-GBM and other institutions [57]. The research selected 1251 cases comprising low-grade glioma (LGG) and glioblastoma (GBM) patients from the provided private institutional dataset. Each MRI scan from the 2000 subjects contained four modalities of T1, T2, T1-contrast enhanced (T1ce) and FLAIR in NIfTI format at dimensions of 240x240x155. The benchmark used for the comparative assessment comprised pre-segmented BraTS2021 scans that received radiology specialist verification for their segmentation. Reference segmentations functioned to improve treatment planning while also providing enhanced tumor evolution understanding through specific identification of three tumor regions: peritumoral edema (ED) enhancing tumor (ET) and necrotic/non-enhancing tumor (NCR).

Evaluation and Performance Metrics

The local objective function of the i -th client is denoted by $f_i(t)$ while x represents the current model parameter and ξ indicates the data point sampled for local training. In these assumptions LOF represents local and SOF demonstrates second-order function smoothness and LH stands for Lipschitz convexity. Lastly, SCOF and COF express objective function convexity while $f(x_1) \geq f(x_2) + (x_1 - x_2)^T \nabla f(x_2)$ indicates the coercive property and CF denotes the existence of a global minimum. BG, BV along BGD determine conditions required to prove convergence. The function characteristics of convexity in MOG are described by two properties: first SCOF and COF while second $f(x_1) \geq f(x_2) + (x_1 - x_2)^T \nabla f(x_2)$ establishes the rules of convexity and the coerciveness of $f(x)$ follows a pattern of $\lim_{x \rightarrow \infty} f(x) \rightarrow \infty$. When CF applies it guarantees the existence of a worldwide minimum for the objective function. The properties of gradients are captured through BG, BV and BGD. This situation emphasizes the need to combine technological expertise with



legal and ethical considerations when approaching such problems. The Proposed Technique relies on the following algorithm.

$$\begin{aligned}
 d_{AHD} (X, Y) &= \left(\frac{1}{X} \sum_{x \in X} \frac{\min_{y \in Y} d(x, y)}{\epsilon X d} \right. \\
 &\quad \left. + \frac{1}{Y} \sum_{y \in Y} \frac{\min_{x \in X} d(x, y)}{\epsilon X d} \right) / 2
 \end{aligned} \tag{Eq (1)}$$

$$\begin{aligned}
 d_{AHD} (2, 31) &= \left(\frac{1}{2} \sum_{x \in X} \frac{\min_{y \in Y} d(2, 31)}{\epsilon X d} \right. \\
 &\quad \left. + \frac{1}{31} \sum_{y \in Y} \frac{\min_{x \in X} d(2, 31)}{\epsilon X d} \right) / 2
 \end{aligned} \tag{Eq (2)}$$

$$\begin{aligned}
 d_{AHD} (4, 41) &= \left(\frac{1}{4} \sum_{x \in X} \frac{\min_{y \in Y} d(4, 41)}{\epsilon X d} \right. \\
 &\quad \left. + \frac{1}{41} \sum_{y \in Y} \frac{\min_{x \in X} d(4, 41)}{\epsilon X d} \right) / 2
 \end{aligned} \tag{Eq (3)}$$

$$\begin{aligned}
 d_{AHD} (2, n) &= \left(\frac{1}{2} \sum_{x \in X} \frac{\min_{y \in Y} d(2, n)}{\epsilon X d} \right. \\
 &\quad \left. + \frac{1}{n} \sum_{y \in Y} \frac{\min_{x \in X} d(2, n)}{\epsilon X d} \right) / 2
 \end{aligned} \tag{Eq (4)}$$

The Average Hausdorff Distance (AHD) is another statistic that defines the shift of two sets of points and is often used to assess a segmentation method, for example, CNN-based Brain Tumor Segmentation.

$$\rho_c = \frac{2a_{12}}{(\mu_1 - \mu_2)^2 + \sigma_1^2 + \sigma_2^2} \tag{Eq (5)}$$

The formula for Cohen's d calculates the impact magnitude in a two-sample t-test, useful for comparing two CNN models' segmentation performance for brain tumors.

μ_1 and μ_2 : Mean performance metrics of two models (e.g., Dice score,



accuracy).

σ_1 and σ_2 : Standard deviations of the performance metrics.

σ_{12} : Covariance between the models' performances.

A higher effect size indicates a more significant performance difference, while zero means no difference. In brain tumor segmentation, Cohen's d helps quantify the magnitude of performance differences between CNN models. Gaussian statistics are used to demonstrate the correlation between these two-reference strategies (variable 1) and alternative techniques (variable 2). The means (μ_1 and μ_2), typical deviations (σ_1 and σ_2), and covariance (σ_{12}) of these variables define them.

R^2

$$= 1 - \frac{\sum_{i=1}^n (Y_i - \hat{Y}_i)^2}{\sum_{i=1}^n (Y_i - \bar{Y})^2} \quad \text{Eq (6)}$$

The measure of prediction success by a CNN model for brain tumor segmentation is determined through the R-squared value calculation.

Y_i : Shows the actual segmentation outcome for the i -th MRI scan. The CNN model generates its predicted segmentation output \hat{Y}_i from an earlier provided scan. \bar{Y} : The average of all actual segmentation results. A higher value of R-squared indicates that the model provides accurate predictions of actual segmentation results. A value of R-squared at 1 indicates complete accuracy in predicting segmented areas. The model completely misses every pattern that contributes to the segmentation outcomes when R-squared equals 0. The model shows the relationship to the segmentation results between 0 and 1. During CNN model evaluation for brain tumor segmentation R-squared proves useful for identifying the right model and represents how well the data is reflected through its value strength. The predictive formula uses Y_i as the reference value Y_i as the projected value and \hat{Y} as the average actual value.



$$\text{RMSE} = \sqrt{\frac{1}{n} \sum_{i=1}^n (Y_i - \hat{Y}_i)^2}$$

Eq (7)

The formula represents one important parameter for evaluating the precision of brain tumor segmentation models is the Root Mean Squared Error (RMSE).

Y_i : The actual label for a voxel in the MRI scan (tumor = 1, non-tumor = 0).

\hat{Y}_i : The predicted label for the voxel from the segmentation model.

n : The total count of voxels within the MRI scan.

The Mean squared error calculates the average value of squared differences between a true object label and a predicted label through an operation that divides the squared label difference by the total number of image Voxel and divides this outcome by the number of scanned images. The division of clustering components reduces the RMSE value below actual values thus allowing the model to generate an enhanced tumor subdivision. CNN-based brain-tumor segmentation networks achieve optimal segmentation using the model that exhibits the lowest RMSE value for performance assessment among models. Y_i represents reference values while $Y_{(i)}$ shows projected values in this formula which uses the value of n for data points.

$$\text{TDI} = \sqrt{(\Delta C)^2 + (\Delta \sigma)^2}$$

Eq (8)

The Total Distance Index (TDI) formula evaluates the accuracy of brain tumor segmentation:

TDI: Measures the distinction between the CNN-segmented tumor and the ground truth.

ΔC : Difference in centroid locations of the segmented tumor versus the ground truth.

$\Delta \sigma$: Difference in standard deviations, reflecting tumor spread.



A lower TDI indicates better segmentation accuracy and helps compare and improve CNN models. The combined results of the two sets of studies provide insightful information about which strategy most closely resembles the reference technique, enabling a reliable and accurate segmentation decision.

$$JSC = \frac{|X \cap Y|}{|X \cup Y|} \quad \text{Eq (9)}$$

Jacquard Measures of the Similarity Coefficient measure the similarity among the predicted tumor boundaries and the reference outlines. Where Y is the reference outline and X is the expected tumor boundary.

$$BDE = \frac{1}{|Y|} * \sum (D(x, Y)) \quad \text{Eq (10)}$$

Boundary Displacement Error measures the average distance between the predicted tumor boundary and the reference outline. Where: x is a point on the predicted tumor boundary, Y is the reference outline, where the distance between x and the closest point on Y is expressed as d(x, Y). The accuracy measures the proportion of the correctly classified instances both true positives and true negatives out of all instances. *TP*: True positives which malicious queries are correctly classified as malicious. *TN*: True Negative which benign queries correctly classified as benign. *FP*: False positive which benign queries incorrectly classified as malicious. *FN*: False Negatives which malicious queries are incorrectly classified. The accuracy, precision, and Recall is defined below:

$$Accuracy = \frac{TP + TN}{TP + TN + FP + FN} \quad \text{Eq (19)}$$

$$Precision = \frac{TP}{TP + FP} \quad \text{Eq (20)}$$



Recall

$$= \frac{TP}{TP + FN}$$

Eq (21)

The F1 Score is the harmonic mean of the Precision and Recall, Which provides a single metric to balance both.

F1 – Score =

$$2 \cdot \frac{Precision \cdot Recall}{Precision + Recall}$$

Eq (19)

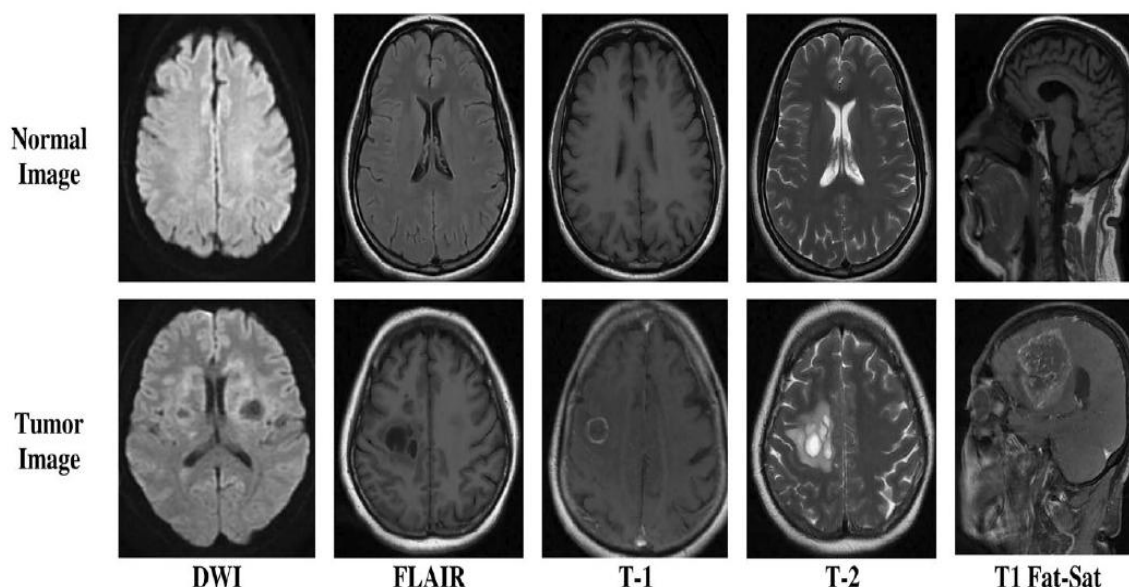


Figure 4. Brain MRI Segmentation with and without Tumor

This study in Figure 4 shows how various approaches execute in automatically segmenting tumors in brain mpMRI images. In Figure 5 brain tumor segmentation comparison utilizes four distinct techniques to segment brain tumors in 1251 people, each with four different sorts of photos. Each scan consists of 155 slices, with three distinct sections identified Edema (ED), necrosis/non-enhancing tumor (NET), and enhancing tumor (ET) are observed on each slice. The dark regions in T1ce images show necrosis, while edema is found in the bright areas in FLAIR and T2 images. To present how well these approaches work, several slices were chosen to show the results. As seen in the figure Every sub-region on a T1ce and T2 MRI scan has a label visible in a single



slice. Necrosis is highlighted in red, the improving blue and yellow for the tumor, and green for the edema. These labels are compared with the ground truth and tumor segments generated by 2D-Vnet, EnsembleUNets, CaPTk, and ResNet50.



Figure 5. Brain MRI Segmentation accuracy curve for train and Test

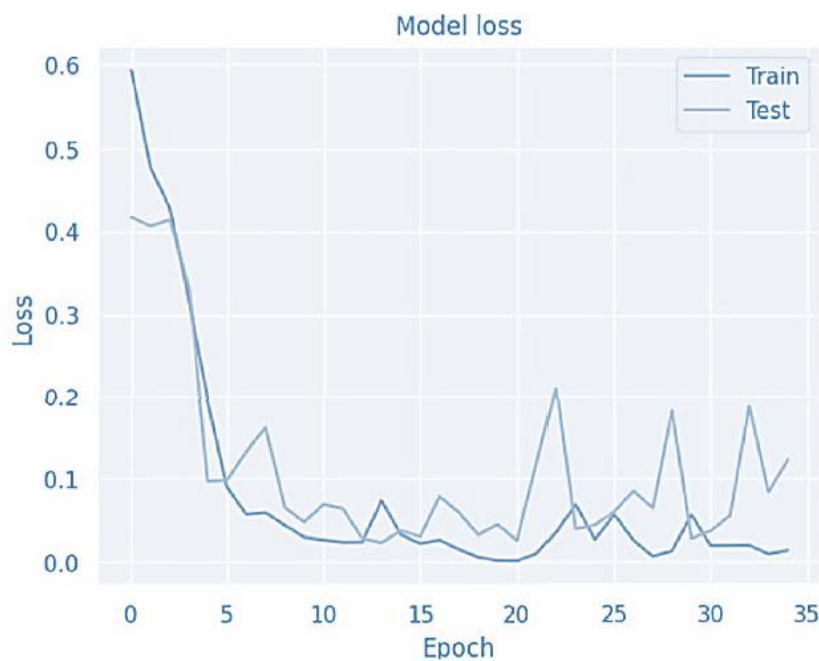


Figure 6. Brain MRI Segmentation Loss curve for train and Test

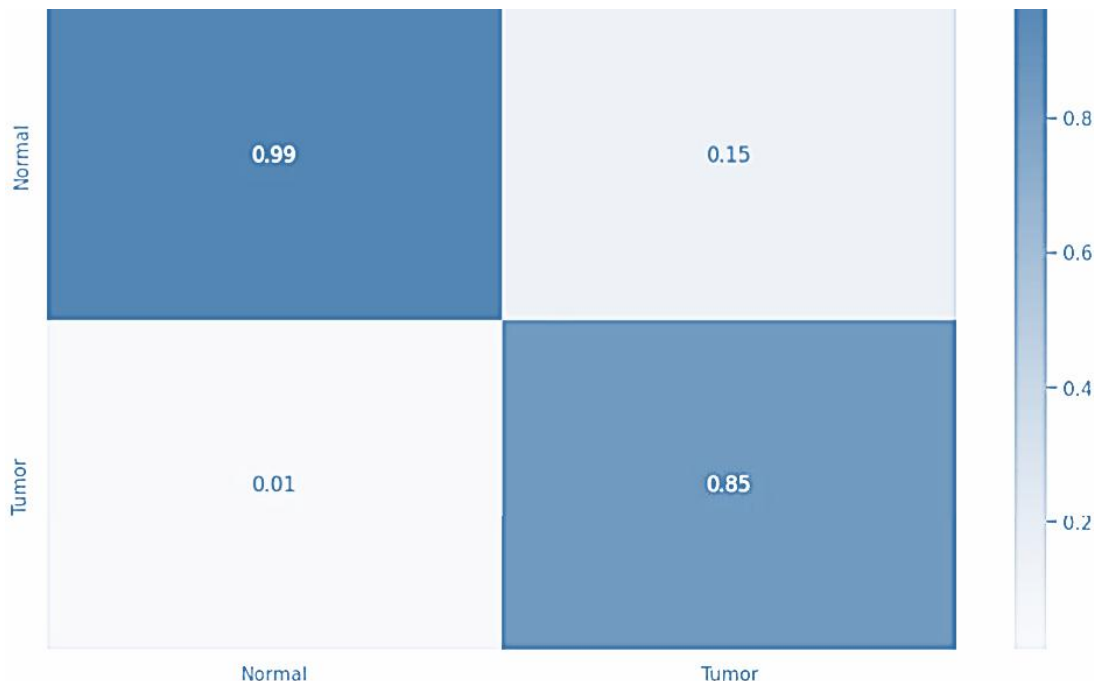


Figure 7. Confusion Matrix of Brain MRI Segmentation with and without Tumor

Sunway Medical Centre uses multimodal MR imaging as its main diagnostic tool for detecting brain tumors. The technique stands as both simple and strong and contributed to the development of radiomics which extracts quantifiable features from MR images. The accuracy of these attributes depends largely on how well tumors get distinguished from their surrounding image area. Research has developed plenty of deep learning approaches for brain tumor segmentation yet a complete evaluation of their performance remains unsettled. The research evaluated several common brain tumor segmentation methods to determine which one delivered optimal results. Our findings are clear. We applied CaPTk, 2DVNet EnsembleUNets and ResNet50 to the BraTS2021 dataset's 1251 samples of T1, T2, T1ce and FLAIR mpMRI images that used an expert-radiologist generated pre-segmented reference image as baseline. The use of Pyradiomics for post-segmentation produced 4852 features from each examined subject.



EnsembleUNets maintained the prime position as the best performer among different statistical metrics through outstanding results across direct tumor segmentation and radiomic feature extraction tasks. The method achieved success because it brings together three unique models (U-Net (3D), MI-U-Net (3D), and MI-U-Net (3D+2D)) using both 3D and 2D image types for precise segmentation. EnsembleUNets shows excellent performance in tumor segmentation which enables better clinical diagnosis and specific tumor classifications and optimized treatment planning, especially for radiation therapy requiring precise tumor outline definition. By being effective the approach could facilitate the connection between radiometric characteristics and genetic information and establish groundwork for developing individualized treatment strategies in disease management research.

Conclusion and Recommendations

Concerning brain tumor recognition in MRI pictures this paper examines four widespread CNN-based systems that handle identification alongside segmentation work along with grouping purposes for glioma medical analysis and treatment preparation tasks. This study presents original findings about the connection between segmentation performance measurements and tumor region radiomic descriptors as previously there were no existing investigations in this area according to the authors. The experimental findings demonstrate that EnsembleUNets delivers optimal results as a superior method among all techniques when examining every performance metric. Researchers and clinical institutions seeking precise correct and time-efficient tumor identification will find EnsembleUNets as a suitable solution. We need to establish methods that will maximize EnsembleUNets' ability to detect tumors with precision since accurate segmentation serves as the foundation for making medical decisions about patient care. The research results establish EnsembleUNets as the best solution for brain tumor detection



together with segmentation and classification from multimodal MRI images.

Funding Statement: The authors received no specific funding for this study.

Conflicts of Interest: The authors declare that they have no conflicts of interest to report regarding the present study.

References

- [1] Islam, M. K., Rahman, M. M., Ali, M. S., Mahim, S. & Miah, M. S. Enhancing lung abnormalities diagnosis using hybrid dcnnvit- gru model with explainable ai: A deep learning approach. *Image Vis. Comput.* 142, 104918 (2024).
- [2] Lee, J.-h., Chae, J.-w. & Cho, H.-c. Improved classification of different brain tumors in mri scans using patterned-gridmask. *IEEE Access* (2024).
- [3] Chung, J., Gulcehre, C., Cho, K. & Bengio, Y. Empirical evaluation of gated recurrent neural networks on sequence modeling. Preprint at arXiv: 1412. 3555 (2014).
- [4] Yang, Y. et al. Early detection of brain tumors: Harnessing the power of gru networks and hybrid dwarf mongoose optimization algorithm. *Biomed. Signal Process. Control* 91, 106093 (2024)..
- [5] Hossain, M. M. et al. Cardiovascular disease identification using a hybrid cnn-lstm model with explainable AI. *Inf. Med. Unlocked* 42, 101370 (2023).
- [6] Ahsan, M. M. et al. Enhancing monkeypox diagnosis and explanation through modified transfer learning, vision
- [7] Mudda, M., Manjunath, R. & Krishnamurthy, N. Brain tumor classification using enhanced statistical texture features. *IETE J. Res.* 68, 3695–3706 (2022).



- [8] Sajid, S., Hussain, S. & Sarwar, A. Brain tumor detection and segmentation in mr images using deep learning. Arab. J. Sci. Eng. 44, 9249–9261 (2019).
- [9] Lan, Y.-L., Zou, S., Qin, B. & Zhu, X. Potential roles of transformers in brain tumor diagnosis and treatment. Brain-X 1, e23 (2023).
- [10] Bhadra, S. & Kumar, C. J. An insight into diagnosis of depression using machine learning techniques: A systematic review. Curr. Med. Res. Opin. 38, 749–771 (2022).
- [11] Ranjbarzadeh, R., Zarbakhsh, P., Caputo, A., Tirkolaei, E. B. & Bendeche, M. Brain tumor segmentation based on optimized convolutional neural network and improved chimp optimization algorithm. Comput. Biol. Med. 168, 107723 (2024).
- [12] Castiglioni, I. et al. Ai applications to medical images: From machine learning to deep learning. Physica Med. 83, 9–24 (2021).
- [13] Gurusamy, R. & Subramaniam, V. A machine learning approach for MRI brain tumor classification. Comput. Mater. Continua 53, 91–109 (2017).
- [14] H. Khan, I. Uddin, A. Ali, M. Husain, "An Optimal DPM Based Energy-Aware Task Scheduling for Performance Enhancement in Embedded MPSoC", Computers, Materials & Continua., vol. 74, no. 1, pp. 2097-2113, Sep. 2023
- [15] Khan, S., Ullah, I., Khan, H., Rahman, F. U., Rahman, M. U., Saleem, M. A., ... & Ullah, A. (2024). Green synthesis of AgNPs from leaves extract of Saliva Sclarea, their characterization, antibacterial activity, and catalytic reduction ability. Zeitschrift für Physikalische Chemie, 238(5), 931-947.
- [16] U. Hashmi, S. A. ZeeshanNajam, "Thermal-Aware Real-Time Task Schedulabilty test for Energy and Power System Optimization using Homogeneous Cache Hierarchy of Multi-core Systems", Journal of Mechanics of Continua and Mathematical Sciences., vol. 14, no. 4, pp. 442-452, Mar. 2023



- [17] Y. A. Khan, F. Khan, H. Khan, S. Ahmed, M. Ahmad, "Design and Analysis of Maximum Power Point Tracking (MPPT) Controller for PV System", *Journal of Mechanics of Continua and Mathematical Sciences.*, vol. 14, no. 1, pp. 276-288, May. 2019
- [18] Ali, M., Khan, H., Rana, M. T. A., Ali, A., Baig, M. Z., Rehman, S. U., & Alsaawy, Y. (2024). A Machine Learning Approach to Reduce Latency in Edge Computing for IoT Devices. *Engineering, Technology & Applied Science Research*, 14(5), 16751-16756.
- [19] Nasir, M. S., Khan, H., Qureshi, A., Rafiq, A., & Rasheed, T. (2024). Ethical Aspects In Cyber Security Maintaining Data Integrity and Protection: A Review. *Spectrum of engineering sciences*, 2(3), 420-454.
- [20] Khan, A. Ali, S. Alshmrany, "Energy-Efficient Scheduling Based on Task Migration Policy Using DPM for Homogeneous MPSoCs", *Computers, Materials & Continua.*, vol. 74, no. 1, pp. 965-981, Apr. 2023
- [21] Abdullah, M., Khan, H., Shafqat, A., Daniyal, M., Bilal, M., & Anas, M. (2024). Internet of Things (IoT's) in Agriculture: Unexplored Opportunities in Cross-Platform. *Spectrum of engineering sciences*, 2(4), 57-84.
- [22] Y. A. Khan, M. Ibrahim, M. Ali, H. Khan, E. Mustafa, "Cost Benefit Based Analytical Study of Automatic Meter Reading (AMR) and Blind Meter Reading (BMR) used by PESCO (WAPDA)", In 2020 3rd International Conference on Computing, Mathematics and Engineering Technologies (iCoMET), IEEE., pp. 1-7, Aug. 2020
- [23] Y. A. Khan, "A high state of modular transistor on a 105 kW HVPS for X-rays tomography Applications", *Sukkur IBA Journal of Emerging Technologies.*, vol. 2, no. 2, pp. 1-6, Jun. 2019
- [24] Khan, S. Ahmad, N. Saleem, M. U. Hashmi, Q. Bashir, "Scheduling Based Dynamic Power Management Technique for offline Optimization of Energy in Multi Core Processors", *Int. J. Sci. Eng. Res.*, vol. 9, no. 12, pp. 6-10, Dec. 2018



- [25] H. Khan, M. U. Hashmi, Z. Khan, R. Ahmad, A. Saleem, "Performance Evaluation for Secure DES-Algorithm Based Authentication & Counter Measures for Internet Mobile Host Protocol", *IJCSNS Int. J. Comput. Sci. Netw. Secur.*, vol. 18, no. 12, pp. 181-185, July. 2018
- [26] Y. A. Khan, "Enhancing Energy Efficiency in Temperature Controlled Dynamic Scheduling Technique for Multi Processing System on Chip", *Sukkur IBA Journal of Emerging Technologies.*, vol. 2, no. 2, pp. 46-53, Jan. 2019
- [27] Khan, K. Janjua, A. Sikandar, M. W. Qazi, Z. Hameed, "An Efficient Scheduling based cloud computing technique using virtual Machine Resource Allocation for efficient resource utilization of Servers", In 2020 International Conference on Engineering and Emerging Technologies (ICEET), IEEE., pp. 1-7, Apr. 2020
- [28] Rahman, M. U., Khan, S., Khan, H., Ali, A., & Sarwar, F. (2024). Computational chemistry unveiled: a critical analysis of theoretical coordination chemistry and nanostructured materials. *Chemical Product and Process Modeling*, 19(4), 473-515.
- [29] Naz, H. Khan, I. Ud Din, A. Ali, and M. Husain, "An Efficient Optimization System for Early Breast Cancer Diagnosis based on Internet of Medical Things and Deep Learning", *Eng. Technol. Appl. Sci. Res.*, vol. 14, no. 4, pp. 15957–15962, Aug. 2024
- [30] Akmal, I., Khan, H., Khushnood, A., Zulfiqar, F., & Shahbaz, E. (2024). An Efficient Artificial Intelligence (AI) and Blockchain-Based Security Strategies for Enhancing the Protection of Low-Power IoT Devices in 5G Networks. *Spectrum of engineering sciences*, 2(3), 528-586.
- [31] H. Khan, M. U. Hashmi, Z. Khan, R. Ahmad, "Offline Earliest Deadline first Scheduling based Technique for Optimization of Energy using STORM in Homogeneous Multi-core Systems", *IJCSNS Int. J. Comput. Sci. Netw. Secur.*, vol. 18, no. 12, pp. 125-130, Dec. 201



- [32] Waleed, A. Ali, S. Tariq, G. Mustafa, H. Sarwar, S. Saif, I. Uddin, "An Efficient Artificial Intelligence (AI) and Internet of Things (IoT's) Based MEAN Stack Technology Applications", Bulletin of Business and Economics (BBE), vol. 13, no. 2, pp. 200-206, July. 2024
- [33] Shah, S. Ahmed, K. Saeed, M. Junaid, H. Khan, "Penetration testing active reconnaissance phase—optimized port scanning with nmap tool", In 2019 2nd International Conference on Computing, Mathematics and Engineering Technologies (iCoMET), IEEE., pp. 1-6, Nov. 2019
- [34] Y. A. Khan, "A GSM based Resource Allocation technique to control Autonomous Robotic Glove for Spinal Cord Implant paralysed Patients using Flex Sensors", Sukkur IBA Journal of Emerging Technologies., vol. 3, no. 2, pp. 13-23, Feb. 2020
- [35] Hassan, H. Khan, I. Uddin, A. Sajid, "Optimal Emerging trends of Deep Learning Technique for Detection based on Convolutional Neural Network", Bulletin of Business and Economics (BBE), vol. 12, no. 4, pp. 264-273, Nov. 2023
- [36] Khan, A. Yasmeen, S. Jan, U. Hashmi, "Enhanced Resource Leveling Indynamic Power Management Technique of Improvement In Performance For Multi-Core Processors" ,Journal of Mechanics of Continua and Mathematical Sciences., vol. 6, no. 14, pp 956-972, Sep. 2019
- [37] Javed, M. A., Anjum, M., Ahmed, H. A., Ali, A., Shahzad, H. M., Khan, H., & Alshahrani, A. M. (2024). Leveraging Convolutional Neural Network (CNN)-based Auto Encoders for Enhanced Anomaly Detection in High-Dimensional Datasets. Engineering, Technology & Applied Science Research, 14(6), 17894-17899.
- [38] Khan, I. Ullah, M. U. Rahman, H. Khan, A. B. Shah, R. H. Althomali, M. M. Rahman, "Inorganic-polymer composite electrolytes: basics, fabrications, challenges and future perspectives", Reviews in Inorganic Chemistry., vol. 44, no. 3, pp. 1-2, Jan. 2024



- [39] Y. A. Khan, U. Khalil, H. Khan, A. Uddin, S. Ahmed, "Power flow control by unified power flow controller", *sss Engineering, Technology & Applied Science Research.*, vol. 9, no. 2, pp. 3900-3904, Feb. 2019
- [40] Ali, M. S., Hossain, M. M., Kona, M. A., Nowrin, K. R. & Islam, M. K. An ensemble classification approach for cervical cancer prediction using behavioral risk factors. *Healthc. Anal.* 5, 100324 (2024).
- [41] Hossain, S., Chakrabarty, A., Gadekallu, T. R., Alazab, M. & Piran, M. J. Vision transformers, ensemble model, and transfer learning leveraging explainable ai for brain tumor detection and classification. *IEEE J. Biomed. Health Inform.* 28, 1261–1272 (2023).
- [42] Padmapriya, S. & Devi, M. G. Computer-aided diagnostic system for brain tumor classification using explainable ai. In *2024 IEEE International Conference on Interdisciplinary Approaches in Technology and Management for Social Innovation (IATMSI) Vol. 2* (ed. Padmapriya, S.) 1–6 (IEEE, 2024).
- [43] Mahim, S. et al. Unlocking the potential of xai for improved alzheimer's disease detection and classification using a vit-gru model.
- [44] Ali, A. M. & Mohammed, M. A. A comprehensive review of artificial intelligence approaches in omics data processing: Evaluating progress and challenges. *Int. J. Math. Stat. Comput. Sci.* 2, 114–167 (2024).
- [45] Lin, D. J., Johnson, P. M., Knoll, F. & Lui, Y. W. Artificial intelligence for mr image reconstruction: An overview for clinicians. *J. Magn. Reson. Imaging* 53, 1015–1028 (2021).
- [46] Wang, S. et al. Advances in data preprocessing for biomedical data fusion: An overview of the methods, challenges, and prospects. *Inf. Fusion* 76, 376–421 (2021).
- [47] Mohan, J., Krishnaveni, V. & Guo, Y. A survey on the magnetic resonance image denoising methods. *Biomed. Signal Process. Control* 9, 56–69 (2014).



- [48] Bhadra, S. & Kumar, C. J. Enhancing the efficacy of depression detection system using optimal feature selection from ehr. *Comput. Methods Biomech. Biomed. Engin.* 27, 222–236 (2024).
- [49] Bernal, J. et al. Deep convolutional neural networks for brain image analysis on magnetic resonance imaging: A review. *Artif. Intell. Med.* 95, 64–81 (2019).
- [50] Salvi, M., Acharya, U. R., Molinari, F. & Meiburger, K. M. The impact of pre-and post-image processing techniques on deep learning frameworks: A comprehensive review for digital pathology image analysis. *Comput. Biol. Med.* 128, 104129 (2021).
- [51] Spieker, V. et al. Deep learning for retrospective motion correction in MRI: A comprehensive review. *IEEE Trans. Med. Imaging* (2023).
- [52] Ali, M. S. et al. Alzheimer’s disease detection using m-random forest algorithm with optimum features extraction. In 2021 1st International Conference on Artificial Intelligence and Data Analytics (CAIDA) (ed. Ali, M. S.) 1–6 (IEEE, 2021).
- [53] Islam, M. K. et al. Melanoma skin lesions classification using deep convolutional neural network with transfer learning. In 2021 1st International Conference on Artificial Intelligence and Data Analytics (CAIDA) (ed. Islam, M. K.) 48–53 (IEEE, 2021).
- [54] Dosovitskiy, A. et al. An image is worth 16x16 words: Transformers for image recognition at scale. Preprint at arXiv: 2010. 11929 (2020).
- [55] Islam, M. K., Rahman, M. M., Ali, M. S., Mahim, S. & Miah, M. S. Enhancing lung abnormalities diagnosis using hybrid dcnnvit- gru model with explainable ai: A deep learning approach. *Image Vis. Comput.* 142, 104918 (2024).
- [56] Lee, J.h., Chae, J.-w. & Cho, H.-c. Improved classification of different brain tumors in mri scans using patterned-gridmask. *IEEE Access* (2024).



[57] Chung, J., Gulcehre, C., Cho, K. & Bengio, Y. Empirical evaluation of gated recurrent neural networks on sequence modeling. Preprint at arXiv: 1412.3555 (2014).